Performance Comparison of Alternating Direction Optimization Methods for Linear-OPF based Real-time Predictive Control

Rahul Gupta[a], Vladimir Sovljanski[a], Fabrizio Sossan[b], Mario Paolone[a]
[a]Distributed Electrical Systems Laboratory, EPFL, Switzerland, [b]PERSEE, Mines ParisTech – PSL, France

***Abstract*—The paper contributes to improving the computational performance of controls of distributed energy resources (DERs) in distribution grids for efficient real-time control and short-term scheduling. The considered setting is a distribution grid with heterogeneous DERs controlled with model predictive control (MPC) to track a dispatch plan at its grid connection point (GCP) subject to DERs' and grid's constraints. The MPC control is first expressed as a quadratic programming (using linearized grid models) and, then, solved with several state-of-the-art alternating direction optimization methods: AMA, ADMM, AADMM (ADMM with adaptive penalty parameter) and their accelerated variants: FAMA, FAADMM, and FAADMM with restart rule. Performance is tested in terms of computational performance, constraints satisfaction, and optimality against the centralized MPC. The case studies are the CIGRE and IEEE benchmark grid for low- and medium voltage systems hosting different numbers of controllable DERs.**

***Index Terms*—Alternating direction optimization, accelerated methods, model predictive control, linear power flow.**

I. Introduction

The wide deployment of renewable power generation in distribution networks requires suitable coordination frameworks to coordinate distributed energy resources (DERs) to support the operations of both the local grid (e.g., voltage control and congestion management [1]–[3]) and the upper-level grid (e.g., dispatch and frequency control [4]–[6]). Frameworks based on model-based optimization and model predictive control (MPC) have been widely advocated in the existing literature to tackle these problems thanks to their feature of explicitly modelling the constraints of the grid and DERs. In order to reduce the complexity associated with solving large problems with many DERs and, in some cases, achieve privacy-preserving formulations that do not require to exchange DERs' full state, distributed optimization methods have been considered. For instance, the work in [7] proposed an MPC formulated with the alternating direction method of multipliers (ADMM) to coordinate between battery storage and curtailable PV plants accounting for the grid constraints. The works in [8], [9] proposed to use distributed optimization to solve the optimal power flow (OPF) problem. Although these methods fulfill their premises in satisfying the grid constraints and achieving the control objectives, the convergence performance was quite poor and it called for accelerated variants based on alternating direction optimization methods [10]. The aspect related to convergence and computation burden is critical in a practical context, especially in real-time controls, where the setpoints have to be issued with refresh rates of tens of seconds.

In this paper, we tackle the problem of improving the computational performance of MPC for grid control by using alternating direction optimization methods. The methods that we survey and of which we demonstrate their applicability are: alternating minimization algorithm (AMA), Fast-AMA (FAMA), ADMM, ADMM with adaptive penalty parameter (AADMM), Fast AADMM (FAADMM), and FAADMM with restart (FAADMM+R). We consider different distribution grids with multiple controllable heterogeneous resources, controlled to track a dispatch plan subject to the local grid's and their operational constraints. Algorithms' performance is evaluated in terms of computation time, feasibility, and dispatch tracking error against the equivalent centralized formulation. For the dominant algorithm, we evaluate how the computational performance scales with the number of controllable resources and on larger power grids.

The rest of the paper is organized as follows. Section II presents the problem to be solved, Section III the decomposition methods, and Section IV the simulation results and the performance comparison. Finally, Section V summarizes the work and presents the conclusions.

II. Problem Statement

We consider the problem of real-time MPC of controllable resources connected to a power distribution network for achieving its dispatchability while accounting for the local grid's constraints. The work was originally proposed in [7] and solved using ADMM by decomposing the control problem into the resources and the grid's ones. In this work, we reformulate it as a quadratic program (QP), allowing us to use the standard alternating direction optimization methods along with their accelerated variations. For the sake of readability, we recall the centralized formulation used in [7].

A. Centralised problem

We consider a generic distribution network, radial or meshed, with n_b nodes and n_l branches. We assume that i) the system is in quasi steady-state and can be modeled by phasors, ii) the system is balanced and can be modeled by means of the direct sequence equivalents although the formulation can be easily extended to an unbalanced system e.g. [11]. Let $\underline{t}$ denote the index of the current time interval, T the number of intervals in the scheduling horizon, Δt the time-resolution and $\mathcal{T} = [\underline{t}, \underline{t}+1, \ldots, T]$ the indices spanning from

Accepted to PowerTech Madrid, 2021.

time $\underline{t}\Delta t$ to the end of scheduling horizon $T\Delta t$. The network interfaces controllable resources with $r \in \mathcal{R} = [1, \dots, R]$ as index and p_t^r, q_t^r as the active and reactive power set-points to determine. Here, p_t^r, q_t^r are collected in vectors $\mathbf{p}_t, \mathbf{q}_t \in \mathbb{R}^{n_b-1}$ respectively. The elements of $\mathbf{p}_t$ and $\mathbf{q}_t$ that correspond to nodes without controllable resources are assumed to be zero. Let $\widehat{p}_t^{\text{disp}}$ be the dispatch plan set-point, and q_t^{gcp} the decision variable for the reactive power at GCP, the scalars p_t^l, q_t^l be the net active and reactive grid losses, and $\mathbf{p}_t^{\text{unc}} \in \mathbb{R}^{n_b-1}$ and $\mathbf{q}_t^{\text{unc}} \in \mathbb{R}^{n_b-1}$ the node-aggregated uncontrollable active and reactive power injections. The objective is to track the dispatch plan using the controllable resources. The problem is to compute the set-points of the controllable resources so as to minimize the weighted sum of operation costs of different controllable resources, $f_r(p_t^r, q_t^r)$, and the dispatch error, δ_t:

$$\underset{\mathbf{p}_t, \mathbf{q}_t, t \in \mathcal{T}}{\text{minimize}} \sum_{r=1}^{R} \sum_{t \in \mathcal{T}} w_r f_r(p_t^r, q_t^r) + \sum_{t \in \mathcal{T}} w_\delta \delta_t^2, \tag{1a}$$

subject to:

$$\mathbf{1}^\top \mathbf{p}_t + \mathbf{1}^\top \mathbf{p}_t^{\text{unc}} + p_t^l = \widehat{p}_t^{\text{disp}} + \delta_t \qquad t \in \mathcal{T} \tag{1b}$$

$$\mathbf{1}^\top \mathbf{q}_t + \mathbf{1}^\top \mathbf{q}_t^{\text{unc}} + q_t^l = q_t^{\text{gcp}} \qquad t \in \mathcal{T} \tag{1c}$$

$$|q_t^{\text{gcp}}| \leq \frac{|\widehat{p}_t^{\text{disp}}|}{\tan(\pi/2 - \theta_m)} \qquad t \in \mathcal{T} \tag{1d}$$

$$\Phi_r(p_t^r, q_t^r) \leq 0 \qquad t \in \mathcal{T}, r \in \mathcal{R} \tag{1e}$$

$$v^{\min} \leq \mathbf{A}_t^{\mathbf{v}} \begin{bmatrix} \mathbf{p}_t \\ \mathbf{q}_t \end{bmatrix} + \mathbf{b}_t^{\mathbf{v}} \leq v^{\max} \qquad t \in \mathcal{T} \tag{1f}$$

$$0 \leq \mathbf{A}_t^{\mathbf{i}} \begin{bmatrix} \mathbf{p}_t \\ \mathbf{q}_t \end{bmatrix} + \mathbf{b}_t^{\mathbf{i}} \leq \mathbf{i}^{\max} \qquad t \in \mathcal{T} \tag{1g}$$

$$\begin{bmatrix} p_t^l \\ q_t^l \end{bmatrix} = \begin{bmatrix} \mathbf{a}_{p_t}^p & \mathbf{a}_{q_t}^p \\ \mathbf{a}_{p_t}^q & \mathbf{a}_{q_t}^q \end{bmatrix} \begin{bmatrix} \mathbf{p}_t \\ \mathbf{q}_t \end{bmatrix} + \begin{bmatrix} b_t^p \\ b_t^q \end{bmatrix} \qquad t \in \mathcal{T} \tag{1h}$$

where $\mathbf{A}_t^{\mathbf{v}} \in \mathbb{R}^{(n_b-1)\times 2(n_b-1)}$, $\mathbf{A}_t^{\mathbf{i}} \in \mathbb{R}^{n_l \times 2(n_b-1)}$, and $\mathbf{a}_{p_t}^p, \mathbf{a}_{q_t}^p, \mathbf{a}_{p_t}^q, \mathbf{a}_{q_t}^q \in \mathbb{R}^{(n_b-1)}$ are the partial derivatives (or sensitivity coefficients) of magnitudes of nodal voltages, lines currents and net losses, respectively, with respect to the nodal power injections and $\mathbf{b}_t^{\mathbf{v}} \in \mathbb{R}^{(n_b-1)}$, $\mathbf{b}_t^{\mathbf{i}} \in \mathbb{R}^{n_l}$, and $b_t^p, b_t^q \in \mathbb{R}$ are known terms of the linear grid model. The sensitivity coefficients are computed with the procedure described in [12] that consists in solving a system of linear equations (with unique solution when the load-flow Jacobian is locally invertible [13]) as a function the grid admittance matrix and the nodal injections around the operating point to linearize. Symbols $v^{\min}$ and $v^{\max}$ are the minimum and maximum voltage limits, and $\mathbf{i}^{\max}$ is a vector with the line ampacities. Symbols w_r and w_δ are weighting coefficients and their values are given in Appendix A. Constraint (1b) bounds the active power flow at the GCP to the dispatch plan with dispatch error δ_t which is minimized in the objective. Eqs. (1c), (1d) impose a lower bound on the power factor $\cos(\theta_m)$ at the GCP by constraining the reactive power flow to the upper-grid layer. Eq. (1e) is inequality constraint that group all the operational constraints of resource r. A practical example is given in the next paragraph. Constraints (1f) and (1g) impose the limits on the nodal voltages and branch currents respectively. Eq. (1h) is the linear model for grid losses. The resource constraint, Φ_r and the objectives, f_r are here made explicit for two cases: a battery energy storage system (BESS) and a PV plant.

1) BESS with four-quadrant power converter: BESS's active and reactive power injections, p_t^b, q_t^b, are subject to the capability curve of its power converter. Approximating it as independent from the voltage of the grid and DC bus, this constraint reads as:

$$0 \leq (p_t^b)^2 + (q_t^b)^2 \leq (S_{\text{max}}^b)^2, \tag{2a}$$

where S_{max}^b is the converter rated power. By modelling the power losses due to non-ideal charging/discharging efficiency as described in [14] (it augments the grid model with a virtual resistive line at the BESS grid connection point), the BESS state-of-energy (SOE) is:

$$\text{SOE}_t = \text{SOE}_{t-1} - p_t^b T_s, \tag{2b}$$

where T_s is the duration of the (piecewise constant) control action. It is subject to

$$a E_{\text{max}}^b \leq \text{SOE}_t \leq (1-a) E_{\text{max}}^b, \tag{2c}$$

where E_{max}^b is the BESS' energy capacity, and parameter a can be designed to fine tune the bounds. The constraints here above form the term $\Phi_b(p_t^b, q_t^b)$ in (1e). The cost function can be designed by the modeller to optimize the resource-specific operational objectives (e.g., ageing, ramping rates, etc.). We choose the norm-2 of the injected active power so as to minimize the BESS' use and implicitly reduce cycle ageing:

$$f_b(p_t^b, q_t^b) = (p_t^b)^2. \tag{2d}$$

2) Curtailable PV plant with controllable reactive power: The goal is minimizing the curtailed (wasted) production and operate near unity power factor to reduce grid losses. With p_t^g, q_t^g as the active and reactive power injections, the cost is:

$$f_g(p_t^g, q_t^g) = \left\{ (p_t^g - \widehat{p}_t^g)^2 + (q_t^g)^2 \right\} \tag{3a}$$

where $\widehat{p}_t^g$ is the (forecasted) PV generation potential.[1] It holds:

$$0 \leq p_t^g \leq \widehat{p}_t^g. \tag{3b}$$

With the power converter capacity, S_{max}^g, the constraint is:

$$0 \leq (p_t^g)^2 + (q_t^g)^2 \leq (S_{\text{max}}^g)^2. \tag{3c}$$

B. QP equivalence

Problem (1)-(3) can be written in standard QP from:

$$\arg\min_{\mathbf{x}} \frac{1}{2} \mathbf{x}^\top \mathbf{D} \mathbf{x} + \mathbf{e}^\top \mathbf{x} \tag{4a}$$

$$\text{s.t.} \quad \mathbf{G}\mathbf{x} \leq \mathbf{h} \tag{4b}$$

where $\mathbf{x}$ is the decision variable, and $\mathbf{D}$, $\mathbf{e}$, $\mathbf{G}$, $\mathbf{h}$ are appropriate matrices and vectors that can be derived from the original problem as described in Appendix A.

[1] Note that the realised PV generation may differ from forecast $\widehat{p}_t^g$; the incurred error can be compensated by the MPC in following timesteps.

To decompose the QP problem, we introduce a new set of slack variables $\mathbf{z}$, and indicator function $\mathcal{I}_+(\mathbf{z})$. Therefore, the QP problem can be reformulated as:

$$\arg\min_{\mathbf{x},\mathbf{z}} \frac{1}{2}\mathbf{x}^\top \mathbf{D}\mathbf{x} + \mathbf{e}^\top \mathbf{x} + \mathcal{I}_+(\mathbf{z}) \tag{5a}$$

$$\text{s.t.} \quad \mathbf{G}\mathbf{x} + \mathbf{z} = \mathbf{h} \tag{5b}$$

The form in (5) is useful as it can be solved by standard algorithms for distributed optimization, as described next.

III. Alternating direction optimization methods

The alternating direction methods are based on the notion of augmented Lagrangian, implemented by introducing a set of Lagrange multipliers $\mathbf{y}$. By defining scaled dual variables $\mathbf{u} = \mathbf{y}/\rho$, the augmented Lagrangian is:

$$L_\rho(\mathbf{x},\mathbf{z},\mathbf{u}) = \frac{1}{2}\mathbf{x}^\top \mathbf{D}\mathbf{x} + \mathbf{e}^\top \mathbf{x} + \mathcal{I}_+(\mathbf{z}) + \frac{\rho}{2}||\mathbf{G}\mathbf{x} - \mathbf{h} + \mathbf{z} + \mathbf{u}||_2^2. \tag{6}$$

This problem is solved by sequential optimization with respect to $\mathbf{x}$ and $\mathbf{z}$ variables, thereafter the duals $\mathbf{u}$ are updated. Here, ρ refers to the penalty parameter. Several methods have been reported in literature to solve this problem, as described next.

1) ADMM: this method was first reported in [15]. The updates of $\mathbf{x}, \mathbf{z}$ and $\mathbf{u}$ are derived by solving the Lagrangian (6) for each variables in sequence. They are simplified to linear matrix operations as follows, the k-th iteration updates are

$$\mathbf{x}^{k+1} = -(\mathbf{D} + \rho\mathbf{G}^\top\mathbf{G})^{-1}[\mathbf{e} + \rho\mathbf{G}^\top(\mathbf{z}^k + \mathbf{u}^k - \mathbf{h})] \tag{7a}$$

$$\mathbf{z}^{k+1} = \max\{0, -\mathbf{G}\mathbf{x}^{k+1} - \mathbf{u}^k + \mathbf{h}\} \tag{7b}$$

$$\mathbf{u}^{k+1} = \mathbf{u}^k + \mathbf{G}\mathbf{x}^{k+1} - \mathbf{h} + \mathbf{z}^{k+1}. \tag{7c}$$

2) AMA: this method was developed in [16]. The iterative steps are simpler than ADMM, but the objective function should be strongly convex (i.e., $\mathbf{D} \succeq \rho\mathbf{I}$, $\mathbf{I}$ being the identity matrix) [10], [17]. In AMA, the $\mathbf{x}$-minimization step does not include the augmented Lagrangian. This results in

$$\mathbf{x}^{k+1} = -\mathbf{D}^{-1}[\rho\mathbf{G}^\top\mathbf{u}^k + \mathbf{e}]. \tag{8}$$

The other two updates are the same as in the ADMM.

3) Fast ADMM (FADMM) and AMA (FAMA) methods: first introduced by Nesterov in [18] for accelerating the gradient-descent algorithm, it was later applied to accelerate the conventional alternating direction algorithms (AMA and ADMM in [10]) by updating the variables with a adaptive scaling [10] as follows:

$$\alpha^{k+1} = \frac{1 + \sqrt{1 + 4(\alpha^k)^2}}{2} \tag{9}$$

$$\widehat{\mathbf{z}}^{k+1} = \mathbf{z}^{k+1} + \frac{\alpha^k - 1}{\alpha^{k+1}}(\mathbf{z}^{k+1} - \mathbf{z}^k) \tag{10}$$

$$\widehat{\mathbf{u}}^{k+1} = \mathbf{u}^{k+1} + \frac{\alpha^k - 1}{\alpha^{k+1}}(\mathbf{u}^{k+1} - \mathbf{u}^k). \tag{11}$$

Eq. (9) introduces a predictor-corrector acceleration factor to the auxiliary and dual variables in (10) and (11). The approach is stable when the objective function is strongly convex. The quantities with $(\widehat{\cdot})$ are used in $\mathbf{x}$ and $\mathbf{z}$ updates as in (7)-(8).

4) Fast ADMM + R: the method is a variant of the last one, where a restart rule is applied based on the combined residual (primal and dual residual error). The steps are the same except a restart rule that is introduced depending on the value of the combined residual $l^k = 1/\rho||\mathbf{y}^k - \widehat{\mathbf{y}}^k||_2^2 + \rho||\mathbf{z}^k - \widehat{\mathbf{z}}^k||_2^2$. If the condition $l^k < \eta l^{k-1}$ is met ($\eta \leq 1$ is a parameter), it proceeds with the same steps as the Fast method (9)-(11), else the variables are reset as in the previous iteration. This step is called restarting and it enforces the monotonicity on the objective (assuring that primal and dual updates are updated in descent direction with respect to residuals). It is recommended to use the restarting step as infrequently as possible, so η is chosen close to 1 (for example, 0.999) [10].

A. Convergence criteria

A typical convergence criterion used in the literature is to stop when the primal and dual residuals reduce below a feasibility tolerance bound. Although the residuals converge to zero at the optimum, a tolerance bound is useful to limit the number of iterations. The primal and dual residuals are $s^k_{\text{pri}} = ||\mathbf{G}\mathbf{x}^k - \mathbf{h} + \mathbf{z}^k||_2$ and $s^k_{\text{dual}} = ||\rho\mathbf{G}^T(\mathbf{z}^{k+1} - \mathbf{z}^k)||_2$ respectively. The convergence criterion is

$$s^k_{\text{pri}} \leq \epsilon^k_{\text{pri}} \text{ and } s^k_{\text{dual}} \leq \epsilon^k_{\text{dual}}, \tag{12}$$

where ϵ^k_{pri} and ϵ^k_{dual} are primal and dual feasibility tolerances as defined in [17] and are given as

$$\epsilon^k_{\text{pri}} = \sqrt{N}\epsilon_{\text{abs}} + \epsilon_{\text{rel}}\max\{||\mathbf{G}\mathbf{x}^k||_2, ||\mathbf{z}^k||_2, ||\mathbf{h}||_2\} \tag{13}$$

$$\epsilon^k_{\text{dual}} = \sqrt{M}\epsilon_{\text{abs}} + \epsilon_{\text{rel}}||\mathbf{G}^\top\mathbf{u}^k||_2. \tag{14}$$

Here, N and M are dimensions of variables $\mathbf{z}$ and $\mathbf{x}$ respectively. The values for ϵ_{abs} and ϵ_{rel} can vary depending upon the application, we set them to be 10^{-4}.

1) Penalty parameter: As known, the convergence speed of the augmented Lagrangian-based methods is sensitive to the penalty parameter ρ [17]. A heuristic-based penalty parameter was used in [19]. The work in [20] proposed an adaptive scheme for updating ρ each iteration based on the recent primal and dual residuals. In this iterative scheme, where the dual and primal residuals are balanced with each other by a factor μ as they both converge to zero, giving the name residual balancing. The iterative scheme for updating ρ is:

$$\rho^{k+1} := \begin{cases} \tau_{\text{incr}}\rho^k & s^k_{\text{pri}} > \mu s^k_{\text{dual}} \\ \rho^k/\tau_{\text{decr}} & s^k_{\text{dual}} > \mu s^k_{\text{pri}} \\ \rho^k & \text{otherwise,} \end{cases} \tag{15}$$

where τ_{incr} and τ_{decr} are multiplying factors. We set μ = 10 and τ_{incr} = 2 and τ_{decr} = 2 as reported in [20].

IV. Simulation Results

A. Simulation setup and input data

1) Setup: The MPC control scheme is applied to the CIGRE low voltage benchmark network [21], which is a three-phase 0.4 kV/400kVA, 18-bus system shown in Fig. 1. The grid hosts 200, 15, 52, 55, 35, and 47 kW of electrical demand (with a power factor of 0.95) at nodes 1, 11, 15, 16, 17, and 18,

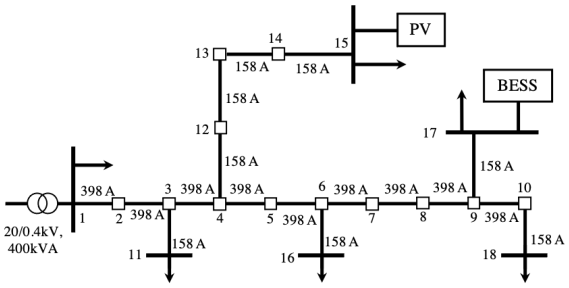

Fig. 1. CIGRÉ low voltage benchmark network [21]

respectively. It is connected with a BESS of 200 kWh/200 kW at node 17 and a curtailable PV plant of 60 kWp at node 15.

The electrical demand and PV generation profiles are shown in Fig 2. These time-series are from real-life measurement collected at the EPFL campus and correspond to the electrical demand of four buildings with rooftop PV installations. The dispatch plan to be tracked, computed with the method in [7], is shown in black in Fig. 2. As it can be seen, the net power at the GCP differs from the dispatch plan, thus the objective of the MPC algorithms is to ensure a power flow at the GCP matching with the dispatch plan by controlling the controllable resources. The real-time operation implements power setpoints with a time resolution $\Delta t = 5$ minutes. The MPC scheduling horizon is 3 hours. The simulations are done on a personal computer with a 2.7 GHz i7 CPU and 16 GB RAM memory.

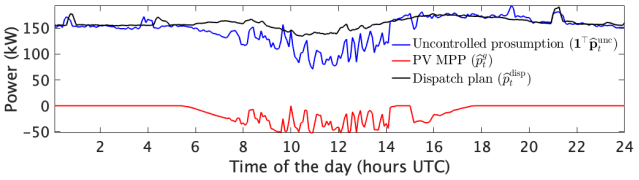

Fig. 2. Active power profiles: the curve in blue displays the load prosumption at the GCP, PV profile is shown in red and the dispatch plan is shown in black.

B. Comparative analysis

We present a performance comparison of MPC among different solving algorithms. We compare the following: AMA, ADMM, FAMA, ADMM with adaptive penalty parameter (AADMM), Fast-AADMM (FAADMM), and FAADMM with restart rule (FAADMM+R). The same tolerance bounds (III-A) are used for all the algorithms. The performance metrics are:

- *convergence speed:* it is measured in time and number of iterations, both expressed in mean, max and min values.
- *tracking error of the dispatch signal:* it is the error between the pre-defined dispatch plan and the net prosumption after MPC. We show root mean square error (RMSE), mean and maximum error;

1) Convergence speed: Table I reports the statistics on convergence time and iterations of the algorithms. We also compare against the centralised problem (1)-(3), solved with the commercial solver MOSEK [22]. It can be seen that FAADMM+R has the minimum mean convergence time compared to other methods, whereas AMA has the worst convergence speed. The ADMM shows better performance than AMA as the latter does not consider augmented Lagrangian in the $\mathbf{x}$-minimization step. By comparing ADMM and AADMM, it can be noted that using the adaptive penalty parameter improves the convergence speed by a factor of 3. The fast methods also improve the convergence speed: FAMA achieves 1/20-th of the AMA's convergence time, FAADMM reduces the mean convergence time of AADMM by 8%. Finally, applying the restart rule further improves the convergence speed of FAADMM by 15%. It can also be observed that the accelerated and adaptive methods score better than the centralised method.

TABLE I
CONVERGENCE SPEED WITH DIFFERENT METHODS FOR ONE DAY OF OPERATIONS.

Method	**Time (sec)**			**Iterations (#)**		
	Min	Mean	Max	Min	Mean	Max
AMA	0.04	51.40	171.5	3405	37895	100000
FAMA	1.8e-3	2.39	10.9	100	2102	9361
ADMM	0.03	2.98	18.9	299	797.8	4868
AADMM	8.9e-3	1.09	3.3	92	314	922
FAADMM	8.5e-3	1.01	3.3	92	314	922
FAADMM+R	3.3e-3	0.86	12.4	54	245.6	3419
Centralised (MOSEK)	1.33	1.51	3.0	n.a.	n.a.	n.a.

2) Dispatch tracking performance: Table II lists the dispatch tracking performance of the MPC solved by different algorithms. It also shows the PV energy curtailed by the MPC to avoid depleting battery's flexibility. The results are analysed for a single day of operation. From the table, it can be seen that the AMA, FAMA and ADMM have similar performances and coincide with the centralised solution. AADMM and FAADMM have better mean error than others but slightly higher maximum error. FAADMM+R performs poorly in terms of the RMSE and maximum dispatch error, and curtails PV slightly more. This is due to the restarting step, which relaxes the solutions leading to early convergence.

TABLE II
TRACKING ERROR WITH DIFFERENT METHODS AND CENTRALISED METHOD FOR ONE DAY OF OPERATIONS.

Method	**Dispatch error (kW)**			**Curtailed PV energy** (%)
	RMSE	Mean	Max	
AMA	0.03	-0.015	0.085	43.13
FAMA	0.03	-0.015	0.085	43.13
ADMM	0.03	-0.015	0.085	43.13
AADMM	0.04	-0.01	0.158	43.09
FAADMM	0.04	-0.01	0.158	43.09
FAADMM+R	0.35	-0.01	1.215	42.95
Centralised (MOSEK)	0.03	-0.015	0.085	43.13

We also present the comparison of dispatch tracking and power-setpoints of the controllable resources by different algorithms and the centralised method in Fig. 3. The plots labeled as "without MPC" refer to the case when MPC is not used. As it can be observed from Fig. 3a, all the algorithms manage to track the dispatch plan successfully and, above

all, the solutions obtained by the decomposition algorithms match with the centralised solution. Fig. 3b shows the state-of-charge evolution and the active power injections of the BESS unit. Fig. 3c shows the active power from the curtailable PV plant. Here, it can be observed that the MPC is able to control BESS and PV (satisfying their operational limits) and achieve a successful dispatch: PV begins curtailing production at 8:00 UTC to anticipate the saturation of BESS flexibility at 14:00 UTC, also helping in tracking the dispatch plan at the GCP. From these analyses, we conclude that FAADMM achieves

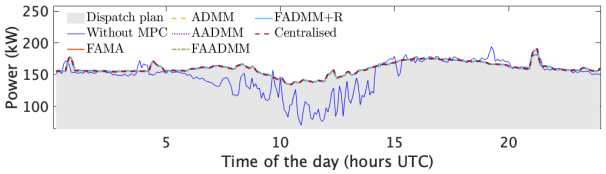

(a) Dispatch plan ($\widehat{p}_t^{\text{disp}}$), active power at the GCP with and without MPC.

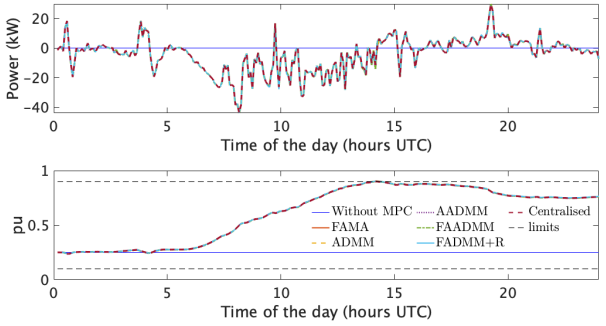

(b) BESS active power injection (p_t^b) (upper panel), and SOC evolution and respective limits (bottom panel).

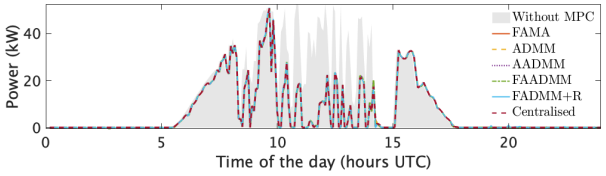

(c) PV active power without ($\widehat{p}_t^g$) and with MPC (p_t^g).

Fig. 3. MPC simulation results with the different methods.

the best performance (both in convergence speed and dispatch error) and it will be now used in a sensitivity analysis.

C. Sensitivity analysis on convergence performance

We evaluate the performance of FAADMM for increasing numbers of decision variables to verify how the convergence time scales, for example, in a larger power grid. We simulate using distributed BESSs units with equal size rating such that the total reservoir size is same for all the cases. Table III shows the convergence time and number of iterations for FAADMM using 2, 3, 4 and 5 BESS units placed at nodes 13, 14, 15, 17 and 18. As it can be observed, the convergence time scales proportionally with the number of controllable units. We also evaluate how the computational performance of FAADMM scales with the number of grid nodes, considering the IEEE34 and IEEE123 balanced systems [23] with two controllable

TABLE III
CONVERGENCE SPEED OF FAADMM FOR INCREASING NUMBERS OF CONTROLLABLE DERS.

BESS		Time (sec)			Iterations (#)		
# units	kWh	Min	Mean	Max	Min	Mean	Max
2	100	6.3e-3	2.63	8.37	92	281.2	813
3	66.7	8e-3	3.47	7.74	82	232.4	444
4	50	6e-3	6.21	18.43	87	373.9	1391
5	40	7.1e-3	8.20	21.8	95	256	613

units: a PV plant and a BESS. Results in Table IV show that the computation time grows proportionally with the number of nodes and, compared to Table III, with a relatively slower rate than for the number of controllable resources.

TABLE IV
CONVERGENCE TIME OF FAADMM WITH LARGER POWER GRIDS.

Network	Controllable resources		Time (sec)		
	BESS	PV plant	Min	Mean	Max
IEEE34	1 MW/2 MWh	480 kWp	9.5e-3	4.43	20.2
IEEE123	2 MW/4 MWh	600 kWp	8.3e-3	9.13	59.5

V. CONCLUSIONS

We have compared the technical and computational performance of different solution methods for distributed optimization problems in the context of dispatching a distribution grid with heterogeneous resources subject to grid constraints formulated with an MPC.

We have shown that, by using linearized models of the grid and realistic models of the controllable resources (generalizable to a wide class of existing systems), the centralized MPC problem can be written in standard quadratic form. In this form, the problem can be readily decomposed using the notion of augmented Langrangian and solved efficiently by applying linear operations iteratively with a number of methods from the literature which are: AMA, ADMM, AADMM (ADMM with adaptive penalty parameter) and their accelerated variants: FAMA, FAADMM, and FAADMM with restart rule.

First, the methods were evaluated on a low-voltage grid with two controllable resources (a curtailable PV plant and a BESS) and uncontrollable stochastic demand, then, the dominant method was used for sensitivity analysis with increasing number of BESSs, and on larger power grids. The performance comparison concerned three aspects: computation time (critical for real-time and near real-time grid control and scheduling), constraints feasibility (which was met in all cases), and dispatch plan tracking. The fast and adaptive ADMM (FAADMM) scored the best computation time (1/3 compared to ADMM) and control performance. The control performance of the decomposition algorithms coincided with the centralised solution (solved by MOSEK). The sensitivity analysis showed that the method scales approximately linearly with the increasing numbers of decision variables supporting the conclusion that this framework can be successfully deployed in actual grids.

APPENDIX

A. QP equivalance of the centralized problem

We derive the matrices of the standard QP problem for the problem (1)-(3) for time interval t.

$$\mathbf{x}_t = \begin{bmatrix} \mathbf{p}_t \\ \mathbf{q}_t \\ \delta_t \end{bmatrix} = \begin{bmatrix} p_t^g \\ p_t^b \\ q_t^g \\ q_t^b \\ \delta_t \end{bmatrix}; \mathbf{D}_t = \text{diag} \begin{pmatrix} w_g \\ w_b \\ w_g \\ 0 \\ w_\delta \end{pmatrix}; \mathbf{e}_t = \begin{bmatrix} -2\widehat{p}_{g,t} \\ 0 \\ 0 \\ 0 \\ 0 \end{bmatrix} \tag{16a}$$

$$\mathbf{G}_t = \begin{bmatrix} \mathbf{1}^\top + \mathbf{a}_{p_t}^p & \mathbf{a}_{q_t}^p & -1 \\ -\mathbf{1}^\top - \mathbf{a}_{p_t}^p & -\mathbf{a}_{q_t}^p & 1 \\ \mathbf{a}_{p_t}^q & \mathbf{1}^\top + \mathbf{a}_{q_t}^q & 0 \\ -\mathbf{a}_{p_t}^q & -\mathbf{1}^\top - \mathbf{a}_{q_t}^q & 0 \\ \mathbf{A}_t^{\mathbf{v}} & & 0 \\ -\mathbf{A}_t^{\mathbf{v}} & & 0 \\ \mathbf{A}_t^{\mathbf{i}} & & 0 \\ -\mathbf{A}_t^{\mathbf{i}} & & 0 \\ \mathbf{G}_t^{\text{pv}} & & 0 \\ \mathbf{G}_t^{\text{bess}} & & 0 \end{bmatrix} \tag{16b}$$

$$\mathbf{h}_t = \begin{bmatrix} -\mathbf{1}^\top \mathbf{p}_t^{\text{unc}} + \hat{p}_t^{\text{disp}} - b_t^p \\ \mathbf{1}^\top \mathbf{p}_t^{\text{unc}} - \hat{p}_t^{\text{disp}} + b_t^p \\ \frac{|\hat{p}_t^{\text{disp}}|}{\tan(\pi/2-\theta_m)} - \mathbf{1}^\top \mathbf{q}_t^{\text{unc}} - b_t^q \\ \frac{|\hat{p}_t^{\text{disp}}|}{\tan(\pi/2-\theta_m)} + \mathbf{1}^\top \mathbf{q}_t^{\text{unc}} + b_t^q \\ v^{\max} - \mathbf{b}_t^{\mathbf{v}} \\ -v^{\min} + \mathbf{b}_t^{\mathbf{v}} \\ -\mathbf{b}_t^{\mathbf{i}} + i^{\max} \\ \mathbf{b}_t^{\mathbf{i}} \\ \mathbf{h}_t^{\text{pv}} \\ \mathbf{h}_t^{\text{bess}} \end{bmatrix} \tag{16c}$$

$$\mathbf{G}_t^{\text{pv}} = \begin{bmatrix} 1 & 0 \\ -1 & 0 \\ \mathbf{G}_{\text{p}} \end{bmatrix}; \ \mathbf{h}_t^{\text{pv}} = \begin{bmatrix} \widehat{p}_t^g \\ 0 \\ \mathbf{h}_{\text{p}}^{\text{pv}} \end{bmatrix} \tag{16d}$$

$$\mathbf{G}_t^{\text{bess}} = \begin{bmatrix} T_s & 0 \\ -T_s & 0 \\ \mathbf{G}_{\text{p}} \end{bmatrix}; \mathbf{h}_t^{\text{bess}} = \begin{bmatrix} (1-a)E_{\max}^b - \text{SOE}_{t-1} \\ -(a)E_{\max}^b + \text{SOE}_{t-1} \\ \mathbf{h}_{\text{p}}^{\text{bess}} \end{bmatrix} \tag{16e}$$

$$\mathbf{G}_{\text{p}} = \begin{bmatrix} -1 & m_1 \\ 1 & -m_1 \\ \vdots & \vdots \\ -1 & m_\beta \\ 1 & -m_\beta \end{bmatrix}; \ \mathbf{h}_{\text{p}}^{\text{pv}} = \begin{bmatrix} c_1^{\text{pv}} \\ c_1^{\text{pv}} \\ \vdots \\ c_\beta^{\text{pv}} \\ c_\beta^{\text{pv}} \end{bmatrix}; \mathbf{h}_{\text{p}}^{\text{bess}} = \begin{bmatrix} c_1^{\text{bess}} \\ c_1^{\text{bess}} \\ \vdots \\ c_\beta^{\text{bess}} \\ c_\beta^{\text{bess}} \end{bmatrix} \tag{16f}$$

For the multi-period formulation, the decision variables and the matrices above are written by concatenating and block-diagonalizing individual time-step quantities, respectively. The SOE constraints should be propagated to the next step. Eq. (16f) approximates the converter capability (2a) and (3c) with β linear constraints with slopes $m_1, \ldots, m_\beta$ and intercepts $c_1^{\text{bess}}, \ldots, c_\beta^{\text{bess}}$ and $c_1^{\text{pv}}, \ldots, c_\beta^{\text{pv}}$. Symbols w_g and w_b are the weights of PV's and BESS's objectives. The weighting coefficient of the tracking objective, $w_\delta = 5e3$, is chosen larger than for PV, $w_g = 1e2$ and BESS, $w_b = 1e2$ to prioritize it.

REFERENCES

[1] P. M. Carvalho *et al.*, "Distributed reactive power generation control for voltage rise mitigation in distribution networks," *IEEE trans. on Power Sys.*, vol. 23, no. 2, pp. 766–772, 2008.

[2] N. C. Scott, D. J. Atkinson, and J. E. Morrell, "Use of load control to regulate voltage on distribution networks with embedded generation," *IEEE Transactions on Power Systems*, vol. 17, no. 2, pp. 510–515, 2002.

[3] E. Dall'Anese *et al.*, "Decentralized optimal dispatch of photovoltaic inverters in residential distribution systems," *IEEE Trans. Energy Conv.*, vol. 29, no. 4, pp. 957–967, Dec 2014.

[4] F. Sossan *et al.*, "Achieving the dispatchability of distribution feeders through prosumers data driven forecasting and model predictive control of electrochemical storage," *IEEE Trans. Sust. Energy*, vol. 7, 2016.

[5] S. A. Pourmousavi and M. H. Nehrir, "Real-time central demand response for primary frequency regulation in microgrids," *IEEE Transactions on Smart Grid*, vol. 3, no. 4, pp. 1988–1996, 2012.

[6] K. Liu, T. Liu, Z. Tang, and D. J. Hill, "Distributed mpc-based frequency control in networked microgrids with voltage constraints," *IEEE Transactions on Smart Grid*, vol. 10, no. 6, pp. 6343–6354, 2019.

[7] R. K. Gupta, F. Sossan, and M. Paolone, "Grid-aware distributed model predictive control of heterogeneous resources in a distribution network: Theory and experimental validation," *IEEE Trans. Energy Conv.*, 2020.

[8] K. Baker, J. Guo, G. Hug, and X. Li, "Distributed mpc for efficient coordination of storage and renewable energy sources across control areas," *IEEE Trans. Smart Grid*, vol. 7, no. 2, pp. 992–1001, 2016.

[9] A. Kargarian *et al.*, "Toward distributed/decentralized dc optimal power flow implementation in future electric power systems," *IEEE Transactions on Smart Grid*, vol. 9, no. 4, pp. 2574–2594, 2016.

[10] T. Goldstein, B. O'Donoghue, S. Setzer, and R. Baraniuk, "Fast alternating direction optimization methods," *SIAM Journal on Imaging Sciences*, vol. 7, no. 3, pp. 1588–1623, 2014.

[11] S. Fahmy, R. Gupta, and M. Paolone, "Grid-aware distributed control of electric vehicle charging stations in active distribution grids," *Electric Power Systems Research*, vol. 189, p. 106697, 2020.

[12] R. Gupta, F. Sossan, and M. Paolone, "Performance Assessment of Linearized OPF-based Distributed Real-time Predictive Control," in *IEEE PowerTech 2019*, Milan, Italy, Jun. 2019.

[13] M. Paolone *et al.*, "Optimal voltage control processes in active distribution networks," IET, Tech. Rep., 2015.

[14] E. Stai, L. Reyes, F. Sossan, J.-Y. Le Boudec, and M. Paolone, "Dispatching stochastic heterogeneous resources accounting for grid and battery losses," *IEEE Trans. Smart Grid*, vol. 9, no. 6, 2018.

[15] R. Glowinski and A. Marroco, "Sur l'approximation, par éléments finis d'ordre un, et la résolution, par pénalisation-dualité d'une classe de problèmes de dirichlet non linéaires," *ESAIM*, vol. 9, pp. 41–76, 1975.

[16] P. Tseng, "Applications of a splitting algorithm to decomposition in convex programming and variational inequalities," *SIAM Journal on Control and Optimization*, vol. 29, no. 1, pp. 119–138, 1991.

[17] S. Boyd *et al.*, "Distributed optimization and statistical learning via the alternating direction method of multipliers," *Foundations and Trends in Machine Learning*, vol. 3, 2011.

[18] Y. Nesterov, "A method of solving a convex programming problem with convergence rate $o(1/k^2)$," in *Soviet Math. Dokl*, vol. 27, no. 2, 1983.

[19] E. Ghadimi *et al.*, "Optimal parameter selection for the alternating direction method of multipliers (admm): quadratic problems," *IEEE Trans. Autom. Control*, vol. 60, no. 3, pp. 644–658, 2014.

[20] B. He, H. Yang, and S. Wang, "Alternating direction method with self-adaptive penalty parameters for monotone variational inequalities," *J. Optimization Theory applicat.*, vol. 106, no. 2, pp. 337–356, 2000.

[21] C. T. F. C6.04.02, "Benchmark systems for network integration of renewable and distributed energy resources," Cigre' International Council on large electric systems, Tech. Rep., July 2009.

[22] Mosek ApS, "The mosek optimization toolbox for matlab manual. version 9.0." 2019.

[23] W. H. Kersting, "Radial distribution test feeders," in *2001 IEEE PES Winter Meeting. Conf. Proc.*, vol. 2. IEEE, 2001, pp. 908–912.